Alec Cao, Cora J. Fujiwara, Roshan Sajjad, Ethan Q. Simmons, Eva Lindroth and David Weld*

Probing Nonexponential Decay in Floquet–Bloch Bands

https://doi.org/10.1515/zna-2020-0020
Received January 18, 2020; accepted February 4, 2020

Abstract: Exponential decay laws describe systems ranging from unstable nuclei to fluorescent molecules, in which the probability of jumping to a lower-energy state in any given time interval is static and history-independent. These decays, involving only a metastable state and fluctuations of the quantum vacuum, are the most fundamental nonequilibrium process and provide a microscopic model for the origins of irreversibility. Despite the fact that the apparently universal exponential decay law has been precisely tested in a variety of physical systems, it is a surprising truth that quantum mechanics requires that spontaneous decay processes have nonexponential time dependence at both very short and very long times. Cold-atom experiments have proven to be powerful probes of fundamental decay processes; in this article, we propose the use of Bose condensates in Floquet–Bloch bands as a probe of long-time nonexponential decay in single isolated emitters. We identify a range of parameters that should enable observation of long-time deviations and experimentally demonstrate a key element of the scheme: tunable decay between quasi-energy bands in a driven optical lattice.

Keywords: Nonequilibrium Dynamics; Non-Markovian Dynamics; Spontaneous Decay; Ultracold Atoms.

1 Introduction

Given the ubiquity of exponential decay, it is surprising that quantum mechanics requires that decay processes to a continuum with a ground state exhibit nonexponential long-time dynamics [1–6]. Classic experiments on the subject include negative results from studies of ^{56}Mn nuclear decay tests [7] and an indirect observation claimed in investigations of ^{8}Be scattering phase shifts [8]. More recently, a variety of physical systems ranging from integrated photonics [9] to Feshbach molecules [10] have emerged as platforms for the exploration of nonexponential decay. Extensive theoretical work has been directed toward nonexponential decay of autoionising resonances in atomic systems [11–13] and laser-induced ionisation effects [14, 15], although this remains at the frontier of experimental feasibility.

Negative ions are often considered in this context, in part due to their simple structure: there is usually only one bound state and a few resonances that simplify the study of laser-induced negative ion photodetachment [14]. Another reason [2, 13] is the possibility of finding broad resonances decaying with a very small energy release, which, as discussed below, should result in a deviation at an earlier time when more is left of the parent. On the experimental side, however, negative ions also pose certain difficulties, especially due to the low target densities available. To our knowledge, no experiments on nonexponential decay in negative ions have been reported.

In a very different physical context, cold atoms in optical lattices can also serve as a probe of decay dynamics [16], as shown, for example, in two seminal experiments. The quantum Zeno effect was first detected using cold sodium atoms in an accelerated optical lattice [17]; more recently, non-Markovian long-time dynamics were observed in an optically dense ensemble of lattice-trapped atoms driven by an applied microwave field [18, 19]. These results demonstrate the promise of degenerate gases in optical lattices for observing long-time modifications to memoryless exponential decay in an ensemble of single emitters.

Here we propose the use of ultracold noninteracting ^{7}Li Bloch oscillating in a tilted modulated optical lattice to directly observe long-time nonexponential interband decay. A schematic of the proposed setup and its relationship to an idealised decay process is presented in Figure 1. While the proposed experiments, in

***Corresponding author: David Weld,** Physics Department, University of California, Santa Barbara, CA, USA, E-mail: weld@ucsb.edu. https://orcid.org/0000-0002-4574-9491
Alec Cao, Cora J. Fujiwara, Roshan Sajjad and Ethan Q. Simmons: Physics Department, University of California, Santa Barbara, CA, USA
Eva Lindroth: Department of Physics, Stockholm University, AlbaNova University Center, Stockholm, Sweden

Published online March 5, 2020

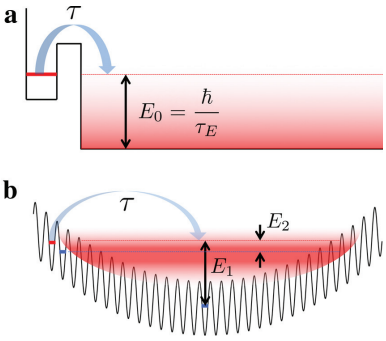

Figure 1: (a) Schematic of a potential in which nonexponential decay is expected. τ is the decay time of the exponential part of the tunnelling process, and $\tau_E = \hbar/E_0$ is the timescale associated with the energy of the decay product. (b) Schematic of proposed optical lattice experiment probing nonexponential decay. E_1 and E_2 are different possible characterisations of the decay product energy.

principle, can be performed in unmodulated lattices (in close analogy to [17] and to pioneering experiments in optical lattice Stückelberg interferometry [20]), we will show that signatures of nonexponential long-time evolution can be greatly enhanced using recently developed tools of Floquet engineering for modification and mapping of band structure [21, 22].

The proposed platform for the exploration of nonexponential decay has several unique advantages. Most important is the extreme tunability afforded by the use of flexible Floquet engineering techniques. Another key advantage, arising from the choice of atomic species, is the presence of broadly Feshbach-tunable interactions in ^{7}Li. In this work, we emphasize the ability to access the single-emitter regime by tuning the scattering length to zero. However, the ability to work at arbitrary scattering length may also enable a future systematic study of the effects of interactions on spontaneous decay.

In Section 2 of this article, we review a heuristic explanation for nonexponential decay based on a simple analysis of the survival probability and the Breit–Wigner energy distribution. We present numerical calculations of the emergence of nonexponential behaviour as a result of imposing the lowest energy bound, revealing decay rate and decay energy as key parameters for experimental observation. In Section 3, we discuss the details and feasibility of the proposed experiment. In particular, we experimentally demonstrate the use of Floquet engineering to engineer the bandgap and tune the decay rate, a key step on the path to realisation of long-time nonexponential decay of an isolated emitter. Section 4 offers conclusions and outlook.

2 Origins of Nonexponential Decay

We begin by recalling a heuristic argument for nonexponential decay that makes no reference to the particular form of the unstable state or decay mechanism [5]. Given some initial state $|\psi_0\rangle$ with Hamiltonian H, the survival or undecayed amplitude $A(t)$ can be calculated as the overlap of the initial state with the time-evolved state $\exp(-iHt/\hbar)|\psi_0\rangle$. For a continuous spectrum, the time-evolved state can be expanded over the complete set of energy eigenstates $|\phi_E\rangle$ as

$$e^{-iHt/\hbar}|\psi_0\rangle = \int \mathrm{d}E|\phi_E\rangle\langle\phi_E|\psi_0\rangle e^{-iEt/\hbar}. \tag{1}$$

Taking the overlap of (1) with $|\psi_0\rangle$ and recognising the initial density of states as $\rho(E) = |\langle\phi_E|\psi_0\rangle|^2$, the survival amplitude is the Fourier transform

$$A(t) = \int_{-\infty}^{\infty} \mathrm{d}E\rho(E)e^{-iEt/\hbar}. \tag{2}$$

The survival probability is $|A^2|$. A simple assumed form for the energy distribution $\rho(E)$ is a Lorentzian or Breit–Wigner distribution:

$$\rho(E) = \frac{\Gamma}{2\pi}\frac{1}{(E-E_0)^2 + (\frac{\Gamma}{2})^2}, \tag{3}$$

where E_0 is the mode, and Γ is the linewidth. Inserting (3) into (2) and squaring yield the familiar result of exponentially decaying survival probability with decay rate $1/\tau = \Gamma/\hbar$.

Nonexponential decay at long times arises from including in this simple argument the fact that real systems necessarily have the lowest energy state, requiring either a truncation of $\rho(E)$ or a bounding of the integral in (2) from below. This alters the form of the survival probability from a pure exponential, giving rise to corrections at long timescales. Figure 2 shows the nonexponential population dynamics that result from imposing such a lower energy bound. The absolute square of $A(t)$ is plotted for varying values of the decay product energy E_0, demonstrating a clear change from almost purely exponential behaviour when E_0 is many linewidths away from the ground state to large oscillations and strongly nonexponential dynamics for small values of E_0. Here, the ground state energy is set to 0. This slower than exponential decay at very long times is well understood theoretically [5, 23], but poses a major challenge for experimental observation due to the small scale of the deviations (note the logarithmic y axis of Figure 2) and the many half-lives

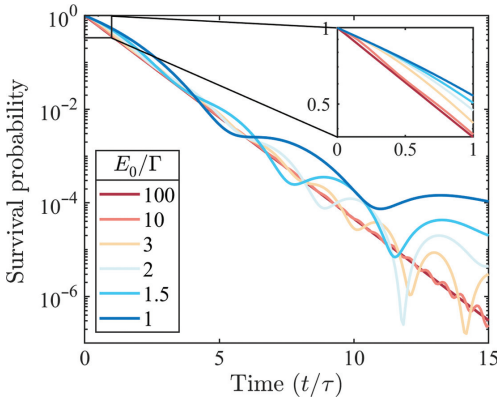

Figure 2: Emergence of nonexponential decay due to truncation of the energy distribution. The survival probability is plotted versus time for various values of E_0, as indicated in the legend. The ground state energy is set to 0. $\hbar$ is set to 1 with time measured in lifetimes τ and energy in linewidths Γ. The inset highlights the largest deviations in the first lifetime.

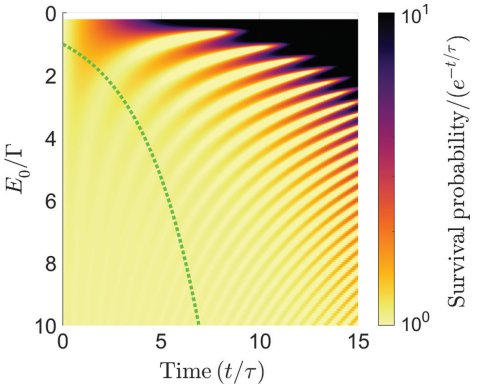

Figure 3: Nonexponential population dynamics as a function of time and the ratio E_0/Γ. Note that the survival probability colour map is normalised to an exponential law in time, with black indicating an order of magnitude population excess with respect to the exponential decay prediction. Dotted green line is the prediction for the onset of nonexponential decay as given by (4).

elapsed before their onset. However, the inset of Figure 2 reveals that significant nonexponential behaviour arises even within the first lifetime when the truncation occurs within a few linewidths of the distribution peak. The scale of these deviations is on the order of 10 %, which should be readily accessible to detection.

It is instructive to compare these results to the prediction of [2] that the timescale τ_L for long time deviations is approximately given by

$$\tau_L \simeq 3\tau \log(E_0\tau/\hbar) = 3\tau \log(E_0/\Gamma), \tag{4}$$

where E_0 is the energy released in the decay. Intuitively, this indicates that τ_L/τ (or E_0/Γ) cannot be much larger than unity in order for there to be a significant remaining population to exhibit nonexponential behaviour. In Figure 3, we map out the numerical integration of (2) for the range of $E_0/\Gamma = 0.2-10$. We also plot the results of (4). While the prediction is qualitatively correct, for $E_0/\Gamma \approx 2-3$ it somewhat overestimates the onset time; there is clear non-Markovian behaviour even within the first time constant. Note the logarithmic scale of the colour bar. Overall, though, Figure 3 confirms the intuitive result of (4) that minimising the decay product energy with respect to the decay rate yields the largest signal for nonexponential behaviour.

In passing, we note that short-time deviations from exponential decay arise from a related but distinct mechanism: the finite expectation value of energy leading to a survival probability with initially vanishing time derivative [24]. This phenomenon underlies the quantum Zeno effect, which was also first realised experimentally with cold atoms [25].

3 Probing Nonexponential Decay in Modulated Optical Lattices

The experimental probe of nonexponential decay we propose here is based on Bloch oscillations of an ultracold atom ensemble through partially avoided band crossings in modulated optical lattices. Our experimental platform consists of a Bose condensate of 10^5 ^{7}Li atoms in a far-red-detuned ($\lambda = 1064$ nm) optical lattice. Interatomic interactions can be eliminated entirely using the shallow zero-crossing below ^{7}Li's broad magnetic Feshbach resonance [26]; this crucially allows us to probe the fundamental question of nonexponential decay of a single emitter. The lattice induces an energy band structure, shown in Figure 4, which can be probed with Bloch oscillations induced by an applied tilt of the harmonic magnetic confinement. In fact, the high tunnelling rate of ^{7}Li enables spatial resolving of different band populations in situ without the use of band maps or time-of-flight imaging [22]. Time-periodic modulation of the lattice depth enables the creation of hybridised Floquet–Bloch bands [21] with a drive-dependent band structure; as argued below, this is a key capability for realistic observation of nonexponential decay.

We begin by considering the use of Bloch oscillations in an undriven lattice as a probe of decay dynamics. In such an experiment, the atoms are adiabatically loaded into the ground band of the lattice and then undergo Bloch oscillations due to the applied force from the inhomogeneous magnetic potential. Ignoring the field curvature, the main correction to the single-band approximation for the Wannier–Stark problem comes from tunnelling between

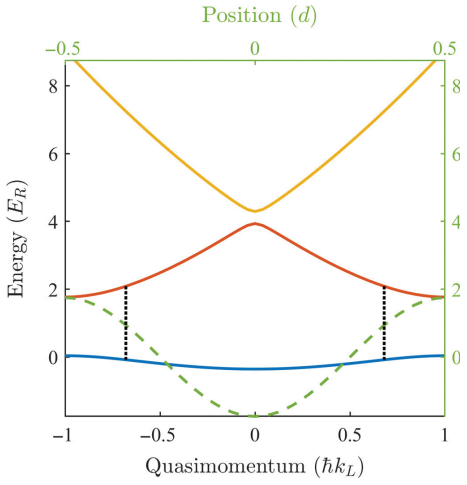

Figure 4: Band structure of a 3.5 E_R deep undriven optical lattice. Solid lines are the lowest three energy bands. Dashed line overlays the lattice potential in position space (top axis). Dotted black line depicts the drive hybridisation scheme used in Figure 5, ignoring coupling to higher bands.

adjacent bands. As the atoms traverse the edge of the Brillouin zone, they have a chance to "decay" by tunnelling across the first bandgap once per Bloch cycle. The feasibility of observing long-time deviations from exponential decay in such an experiment can be quantitatively estimated using a Landau–Zener model of interband tunnelling [27]. Semiclassically, the probability of tunnelling across the n^{th} bandgap Δ_n in a single Bloch cycle is

$$P_n = \exp\left[-\frac{\pi^2}{2}\frac{\Delta_n^2}{hf_B\frac{\partial}{\partial q}|\mathcal{E}_n - \mathcal{E}_{n-1}|}\right], \tag{5}$$

where f_B is the Bloch frequency, and $\mathcal{E}_n$ is the dispersion of the n^{th} band in the free particle limit, indexed with $n = 0$ as the ground band. The derivative with respect to the undimensionalised quasi-momentum ($q = k/k_L$ and $k_L = 2\pi/\lambda$) is evaluated at the point of avoided crossing. By modelling the decay as a discrete process happening once per Bloch cycle and then taking a continuum limit, the effective tunnelling rate across the n^{th} bandgap is approximated as

$$\frac{1}{\tau} \approx f_B \log\left(\frac{1}{1-P_n}\right). \tag{6}$$

In a shallow lattice, tunnelling between all excited bands is large, and we can treat them as a continuum, so we need to focus only on tunnelling across the first bandgap. In calculating the probability P_1 to tunnel out of the ground band, we have $\frac{\partial}{\partial q}|\mathcal{E}_1 - \mathcal{E}_0| = 4\ E_R$ evaluated at the Brillouin zone edge $q = 1$, where the recoil energy is $E_R = \hbar^2 k_L^2/2m$ with $m = 7$ amu. Equations (5) and (6) reveal two important parameters for optimising the decay rate of static Bloch oscillations: the bandgap Δ_1 and the Bloch frequency f_B. These cannot be tuned arbitrarily, although the bandgap is minimised for low lattice depths, and the Bloch frequency is maximised for large magnetic field gradients. Our experiment can reliably achieve Bloch frequencies $f_B \approx 100$ Hz and minimum usable lattice depths of around $1E_R$, yielding $\Delta_1 \simeq 0.5\ E_R$. Inserting these values into (5) and (6) reveals that the resulting tunnelling probability will be minimal: $P_1 \sim 10^{-5}$, leading to a decay time $\tau \sim 10^3$ s. Clearly more tunability is needed to reach a regime where the predicted long-time deviations from exponential decay can be observed. One route could be to use the much stronger gradients attainable in accelerating lattices, but this intrinsically limits the attainable measurement time as the atoms leave the region of interest. A more flexible possibility is the use of Floquet engineering to tune the bandgap.

Thus motivated, we consider the addition of time-periodic lattice depth modulation to the experimental protocol outlined above. Resonant coupling of two static bands by such a modulation generically creates a hybrid quasi-energy band structure featuring at least one new gap, of a size determined by drive strength rather than lattice depth [21]. Figure 5b shows calculated quasi-energy band structure near such a gap, for several different values of the drive strength. Tunnelling across this tunable gap during a Bloch oscillation in a modulated lattice can realize a much more controllable decay process, in which the decay time can be tuned independently of lattice depth and potential tilt.

To demonstrate this central element of the proposed realisation of nonexponential decay, we have experimentally measured tunable Landau–Zener decay in a Floquet-engineered quasi-energy band structure. Figure 5 presents an experimental measurement of the Landau–Zener decay probability of (5) across a Floquet-tunable bandgap as a function of drive strength, for the case of resonant driving between the lowest two energy bands. Images of the two spatially resolved band populations after half a Bloch period in the amplitude-modulated lattice are shown in Figure 5a, and the calculated band crossing in the quasi-energy picture is shown in Figure 5b. The spatial separation between "decayed" and "undecayed" populations is a consequence of position-space Bloch oscillations in the two different band dispersions [22]. Plotting the fraction of undecayed atoms that remain in the ground band, we measure a tunable decay in qualitative agreement with the Landau–Zener tunnelling theory of (5), as shown in Figure 5b. Deviations of the data from theory may be the result of uncertainty in the lattice depth or inhomogeneity

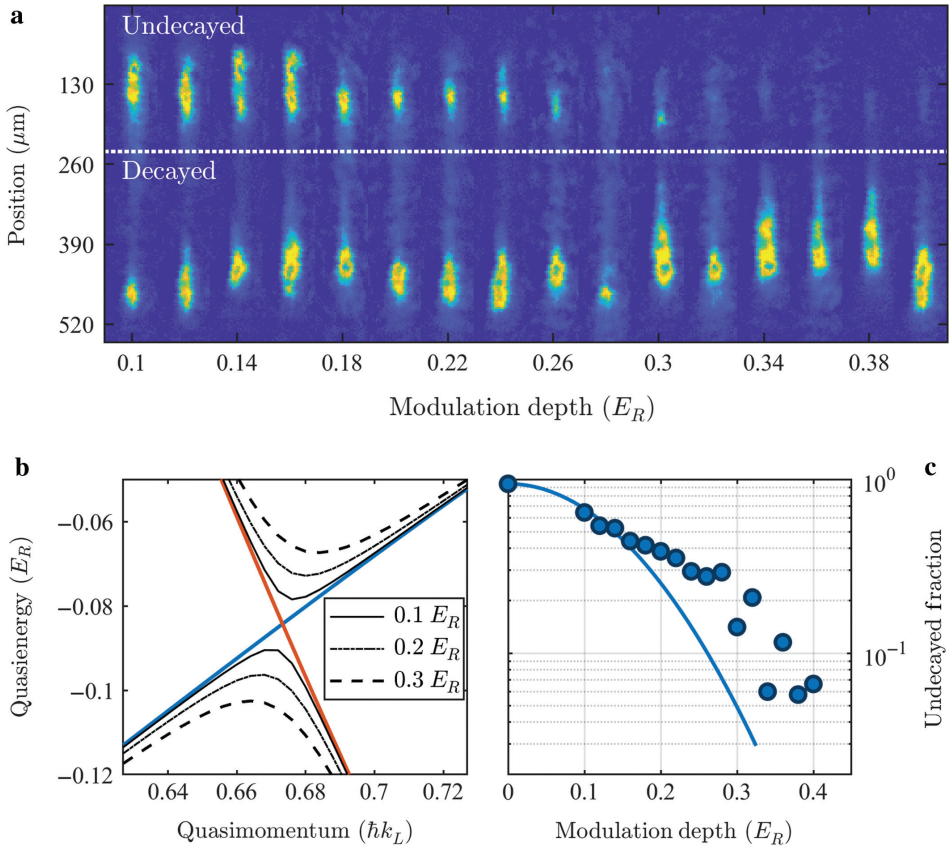

Figure 5: Experimental demonstration of Floquet-tunable decay. (a) Images of a sample of cold lithium atoms after a single Landau–Zener tunnelling event during a Bloch oscillation in a quasi-energy band. The "undecayed" upper clouds are those that remain in the ground band of the corresponding undriven system. The lattice depth is 3.5 E_R, the modulation frequency is 55 kHz, and the Bloch frequency is 27.8 Hz. (b) Calculated quasi-energy band structure around the avoided crossing for different modulation depths (indicated in legend). Note the drive-tunable gap. (c) Undriven ground band fraction as a function of drive strength. Solid theory line is calculated from (5).

of the force. Note that, in this case, it is actually the atoms that fail to undergo the tunnelling event that correspond to the decayed population. To obtain a decay rate then, we must actually subtract (5) from 1. In any case, these results demonstrate the capacity to use lattice modulation to tune the tunnelling probability over a wide range, including an enhancement of roughly four orders of magnitude over the tunnelling probability in a static band for equivalent conditions. Crucially, this allows Γ to approach our achievable Bloch frequencies of up to 100 Hz, allowing for reasonable experimental run times and detectable nonexponential dynamics.

4 Conclusion

We have proposed a measurement of nonexponential decay of individual emitters that is based on interband tunnelling of cold atoms during a Bloch oscillation in a Floquet-engineered quasi-energy band. A simple theoretical treatment of expected dynamics indicates that deviations from exponential decay should be measurable. Preliminary experimental tests of the proposed tunable decay mechanism demonstrate widely tunable decay rates and the feasibility of the underlying concept. These results lay the groundwork for realising a new experimental probe of universal non-Markovian evolution and open up new possibilities for exerting quantum control over an irreducible element of nonequilibrium quantum dynamics.

Acknowledgements: We thank Andrey Kolovsky, Toshi Shimasaki, and Peter Dotti for useful discussions and Jeremy Tanlimco and Jared Pagett for experimental assistance. E.L. acknowledges support from the Knut and Alice Wallenberg Foundation and from the Swedish Research Council (Funder Id: http://dx.doi.org/10.13039/501100004359, 2016-03789). D.W. is grateful for hospitality provided by the guest researcher program of the Wallenberg Centre for Quantum Technology

and acknowledges support from the National Science Foundation (Funder Id: http://dx.doi.org/10.13039/100000001, CAREER 1555313), the Army Research Office (PECASE Funder Id: http://dx.doi.org/10.13039/100000183, W911NF1410154 and Funder Id: http://dx.doi.org/10.13039/100000183, MURI W911NF1710323), and the University of California Multicampus Research Programs and Initiatives (MRP19-601445). D.W. and R.S. acknowledge support from the UCSB NSF Quantum Foundry through Q-AMASE-i program award Funder Id: http://dx.doi.org/10.13039/100000001, DMR-1906325.

References

[1] J. J. Sakurai and J. Napolitano, Modern Quantum Mechanics, Addison-Wesley, San Francisco, CA 1994.
[2] P. Greenland, Nature **335**, 298 EP (1988).
[3] L. Khalfin, JETP **6**, 1371 (1957).
[4] R. Winter, Phys. Rev. **123**, 1503 (1961).
[5] L. Fonda, G. C. Ghirardi, and A. Rimini, Rep. Prog. Phys. **41**, 587 (1978).
[6] P. Knight, Phys. Lett. A **61**, 25 (1997).
[7] E. B. Norman, S. B. Gazes, S. G. Crane, and D. A. Bennett, Phys. Rev. Lett. **60**, 2246 (1988).
[8] N. G. Kelkar, M. Nowakowski, and K. P. Khemchandani, Phys. Rev. C **70**, 024601 (2004).
[9] A. Crespi, F. V. Pepe, P. Facchi, F. Sciarrino, P. Mataloni, et al., Phys. Rev. Lett. **122**, 130401 (2019).
[10] F. Pepe, P. Facchi, Z. Kordi, and S. Pascazio, Phys. Rev. A **101**, 013632 (2020).
[11] C. A. Nicolaides and D. R. Beck, Phys. Rev. Lett. **38**, 683 (1977).
[12] S. Druger and M. Samuel, Phys. Rev. A **30**, 640 (1984).
[13] C. A. Nicolaides and T. Mercouris, J. Phys. B-At. Mol. Opt. **29**, 1151 (1996).
[14] K. Rzazewski, M. Lewenstein, and J. H. Eberly, J. Phys. B-At. Mol. Phys. **15**, L661 (1982).
[15] A. M. Ishkhanyan and V. P. Krainov, Laser Phys. Lett. **12**, 046002 (2015).
[16] M. Holthaus, J. Opt. B-Quantum S. O. **2**, 589 (2000).
[17] S. Wilkinson, C. F. Bharucha, M. C. Fischer, K. W. Madison, P. R. Morrow, et al., Nature **387**, 575 (1997).
[18] L. Krinner, M. Stewart, A. Pazmiño, J. Kwon, and D. Schneble, Nature **559**, 589 (2018).
[19] M. Stewart, L. Krinner, A. Pazmiño, and D. Schneble, Phys. Rev. A. **95**, 4512 (2017).
[20] S. Kling, T. Salger, C. Grossert, and M. Weitz, Phys. Rev. Lett. **105**, 215301 (2010).
[21] C. J. Fujiwara, K. Singh, Z. A. Geiger, R. Senaratne, S. V. Rajagopal, et al., Phys. Rev. Lett. **122**, 010402 (2019).
[22] Z. A. Geiger, K. M. Fujiwara, K. Singh, R. Senaratne, S. V. Rajagopal, et al., Phys. Rev. Lett. **120**, 213201 (2018).
[23] K. Urbanowski, Eur. Phys. J. D **54**, 25 (2009).
[24] L. Khalfin, JETP **8**, 106 (1968).
[25] M. Fischer, B. Gutiérrez-Medina, and M. Raizen, Phys. Rev. Lett. **87**, 040402 (2001).
[26] S. E. Pollack, D. Dries, M. Junker, Y. P. Chen, T. A. Corcovilos, et al., Phys. Rev. Lett. **102**, 090402 (2009).
[27] M. Glück, A. R. Kolovsky, and H. J. Korsch, Phys. Rep. **366**, 103 (2002).